Biochimica et Biophysica Acta, 462 (1977) 63–72

BBA 47359

EXCITED STATE ANNIHILATION IN THE PHOTOSYNTHETIC UNIT

G. S. BEDDARD and G. PORTER

Davy Faraday Research Laboratory of The Royal Institution, 21 Albemarle Street, London W1X 4BS (U.K.)

(Received February 3rd, 1977)

SUMMARY

The kinetics of the in vivo fluorescence decays and fluorescence yields, as a function of excitation intensity, have been analysed with a model using excited state annihilation and time-dependent quenching processes. Triplet states, formed in the singlet-singlet annihilation processes, account for additional quenching of singlet states and the persistence of annihilation at longer times than the fluorescence lifetime. Together these processes give a satisfactory account of existing experimental data of the intensity dependence of fluorescence in vivo.

INTRODUCTION

The intensity dependence of fluorescence yields [1] and lifetimes [2–4] in the photosynthetic unit (PSU) has been attributed to bimolecular annihilation of the excited states [1–8]. This annihilation process is possible because of the large number of excitations produced within a few picoseconds as a result of intense laser excitation. Consequently, the fluorescence lifetime may be shorter than that measured by conventional nanosecond flash lamp techniques. Here we use a simple model of the quenching process in order to match the fluorescence decays and relative yields at various excitation intensities.

Quenching processes in the PSU

It is well established that Förster type energy migration is the most important process transporting electronic excitation energy from the carotenes and chlorophylls of the light harvesting network to the photosynthetic reaction centres [9]. The migration occurs as a hopping process rather than as a delocalised exciton, since coherence is rapidly lost as a result of vibrational redistribution and relaxation in the first excited singlet state. To effect transfer of energy the donor fluorescence and acceptor absorption spectra must overlap, the donor molecule can then give up its energy anywhere in its allowed fluorescence spectrum and the acceptor will receive this anywhere in its allowed absorption spectrum. The pairwise transfer rate between chlorophylls in vivo is in the 10^{11}–10^{12} s^{-1} range, the exact value depending upon the relative orientation and distance apart of the two dipoles.

When two or more photons are absorbed within a few picoseconds into the same PSU then the probability of two excited states coming close enough to annihilate one another becomes significant. A number of processes can occur as a result of singlet-singlet annihilation, these are:

$$S_1+S_1 \rightarrow S_0+S_1^{\#} \rightarrow S_0+S_1 \quad (1)$$

$$S_1+S_1 \rightarrow T+T \quad (2)$$

$$S_1+T \rightarrow (T)S_0+T \quad (3)$$

$$T+T \rightarrow S_0+S_1 \quad (4)$$

These reactions are preceded by energy migration of the excited species towards one another. In these equations S_1, S_0 and T are the first excited singlet, ground state and triplet of chlorophyll, respectively. $S_1^{\#}$ represents a vibrationally excited S_1 state which will relax rapidly to S_1. These reactions are known to occur in solution with a number of molecules, particularly aromatics [10, 11]. When the molecules are excited into the second singlet the possibility of S_2+S_0 and S_2+S_1 transfer processes must also be considered. The latter process occurs at a rate comparable to internal conversion from S_2 to S_1 [12].

In the PSU Reactions 1–4 probably occur via Förster energy transfer [13, 14] as the characteristic distance R_0 may be large. A value for R_0 of 4.8 nm has been calculated [13, 14] for process 3 compared to 6.5 nm for S_1 to S_0 transfer in lipid bilayers [15]. The values for Reactions 1, 2 and 4 have not, to our knowledge, been calculated (due to lack of appropriate absorption or emission spectra) but it is not unreasonable to assume that the values are similar to that for S_1 to T transfer. The similarity of singlet-singlet and triplet-triplet absorption spectra in pheophytins and some porphyrins [16] supports this suggestion. The importance of knowing the exact rates for Reactions 1–4 is somewhat diminished when we consider that the rate for the energy migration, which brings the excited states into the possible quenching configurations, is not known accurately. The rate for chlorophyll singlet migration in a lipid bilayer vesicle may be estimated from the chlorophyll fluorescence lifetimes measured as a function of chlorophyll concentration. The combined rate of the migration and quenching step is given by $(1/\tau_Q - 1/\tau)/Q$, where τ_Q is the fluorescence lifetime in the presence of quenchers at concentration Q and τ the lifetime in the absence of quenchers. A rate constant of $5 \cdot 10^{10}$ $dm^3 \cdot M^{-1} \cdot s^{-1}$ was measured for the migration and quenching step at 0.1 M chlorophyll concentration and assuming that quenching occurs via statistical pair traps [15] at a separation of 1 nm. As the average concentration of chlorophyll in the chloroplast is 0.1 M [9] the quenching step is fast ($> 10^{12}$ s^{-1}) so that migration is the rate-determining step. Reactions 1 and 2 will have similar rates since singlet migration is the rate-determining process. The rate constant for Reaction 4 is possibly less than for singlet migration as the Förster characteristic distance R_0 is expected to be less than for the corresponding singlet step. This is found in general for triplet migration [10, 11, 13, 14].

The rate of Reaction 3, together with the mutual diffusion coefficient of the molecules, has been estimated for chlorophyll in solution [13, 14] as $2.7 \cdot 10^{10}$ $dm^3 \cdot M^{-1} \cdot s^{-1}$. To use this value to describe S-T migration and quenching in the PSU we have to assume a similar value for the diffusion coefficient of the energy

migration as for molecular diffusion in solution. Most probably the value is larger in the PSU but not greatly so as the rate for Reaction 3 is similar to that estimated for Reaction 1. Direct singlet to triplet intersystem crossing is a slow process ($10^8\ s^{-1}$) and is not an important source of triplets following single picosecond pulse excitation. The fluorescence decays before the triplets produced by this process can build up a significant population. This is not the case with excitation using a pulse train such as that from a mode locked laser, as now the triplet population can become significant. The quenching produced by the triplets may explain the apparent absence of intensity effects when the fluorescence decays are measured in the middle of the pulse train [17].

In order that we may analyse the fluorescence yield and decay curves at various incident light intensities, we shall initially make the simplifying assumption that only Reactions 1 and 2 contribute to the fluorescence quenching. We also assume that ground state depletion, direct excited state absorption and stimulated emission are all negligible. The rate expression is then

$$dn/dt = I(t) - an - bn^2 \tag{5}$$

where $I(t)$ is the excitation term which is a delta function on the time scale of the fluorescence, n is the number of excited singlets/PSU, a is the rate constant of all unimolecular processes (fluorescence, internal conversion, intersystem crossing and quenching by the reaction centre) and b is the bimolecular rate constant of singlet-singlet annihilation. The initial number of excited states is n_0 and we assume that these are produced instantaneously on the time scale of the decay of the singlets by I_0 photons/cm^2 per s. The (normalised) fluorescence intensity at time t and quantum yield Φ are given by Eqns. 2 and 3, respectively.

$$n(t)/n(0) = a/((a+bn_0)\exp(at) - bn_0) \tag{6}$$

$$\Phi = K_f/n_0 b \cdot \log_e(1+bn_0/a) \tag{7}$$

where K_f is the excited singlet radiative decay rate. Fig. 1 shows how Φ (Eqn. 7) behaves as a function of n_0, the average number of hits on the PSU. Also plotted

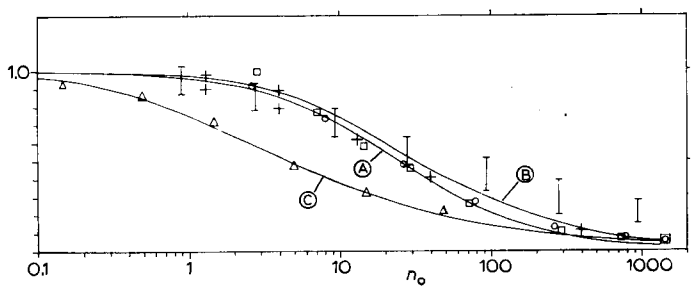

Fig. 1. Relative fluorescence yield Φ/Φ_0 versus the average number of hits on the PSU, n_0. Curve A, Eqn. 7 ($\alpha = 2.5 \cdot 10^9\ s^{-1}$, $\beta = 2.5 \cdot 10^8\ dm^3 \cdot m^{-1} \cdot s^{-1}$). Curve B, Eqn. 10 ($\alpha = 7 \cdot 10^4\ s^{-\frac{1}{2}}$, $\beta = 2.2 \cdot 10^5\ dm^3 \cdot m^{-1} \cdot s^{-\frac{1}{2}}$) and Curve C, Eqn. 7A. Experimental data points: △, Mauzerall, [18, 19]; Campillo et al. [1]; × and ○, Geacintov and Breton, [6, 7]; (683 and 735 nm, respectively); and □, Monger et al. [8]. The data points are superimposed on to curve B to allow a comparison between the data to be made. n_0 refers only to the smooth curves and not to the data points.

are the data of Campillo et al. [1] for *Chlorella*, the data of Geacintov and Breton [6, 7] for chloroplasts and of Monger et al. [8] for bacterial chromatophores. Within the fluctuations of the data points a good fit is obtained. In this figure the various data points have been displaced along the abscissae so that a comparison of all the data points with the calculated values can be made. Consequently the value of n_0 refers only to the calculated curves and not necessarily to the number of hits on the PSU. The reasons why the different organisms studied have different half yield values ($\Phi = 0.5$) is unclear but it may reflect the different size and organisation in the various photosynthetic units. The data of Campillo et al. [1] fit less well at high light intensities owing to a residual yield of 20 % of the maximum yield, this effect is also apparent in the data of Porter et al. [24]. The possible reasons for this have been discussed elsewhere [1, 2].

So far we have assumed delta pulse excitation of the system, such as from a picosecond laser pulse but, by using a laser pulse of 7 ns Mauzerall [18, 19] has observed a similar decrease in fluorescence yield to that described here. He explains the decrease in yield by using a Poisson distribution (to describe the number of hits on the PSU) together with random processes in either time or space. He considers that the decrease in yield is more consistent with events in the spatial than time domain [18, 19].

As the fluorescence decay is at least 10 times less than the duration of the laser pulse used we may apply steady-state conditions to Eqn. 5 to obtain the yields Φ_s*. This is given by Eqn. 7A

$$\Phi_s = K_f a/2bn_0(-1+(1+4bn_0/a^2)^{\frac{1}{2}}) \tag{7A}$$

In Fig. 1, curve C shows how Φ_s varies with n_0, also plotted are the data of Mauzerall [18, 19] (as triangles). An adequate fit to the data is obtained using Eqn. 7A indicating that even with long laser pulses the annihilation processes can describe the relative yields as a function of laser intensity. Since this work was completed similar equations to 7 and 7A have been used by Swenberg et al. [20] to describe the annihilation processes. The experimental data of Monger et al. [8] in which a 15 ns laser pulse was used for excitation is found to be better described by Eqn. 7 than 7A. The reasons for this are not known but it is possible that during the long laser pulse used intersystem crossing to produce triplets could be an important process. The effect of triplet states is discussed in a later section.

Analysis using time-dependent quenching processes

At both low and high light intensities, using dark adapted *Chlorella* [2] and subchloroplast particles, Porter et al. [3, 4] observed that the fluorescence intensity, at time t, was given by $n(t) = I\exp(-Dt-Et^{\frac{1}{2}})$, with I an arbitrary constant. The contribution to the decay of the term Dt is much smaller than that of the other term and the Dt term could be ignored (see Fig. 2). This decay law is similar to that occurring in fluid solution where the rate of diffusional quenching is time dependent [21, 22]. Except at very short times this rate is proportional to $t^{-\frac{1}{2}}$. The dependence

* This assumption ignores the fluorescence on the rising and falling edges of the laser pulse. A more accurate analysis would involve the convolution of the fluorescence decay with the laser pulse profile. In this equation n_0 is the number of hits/laser pulse.

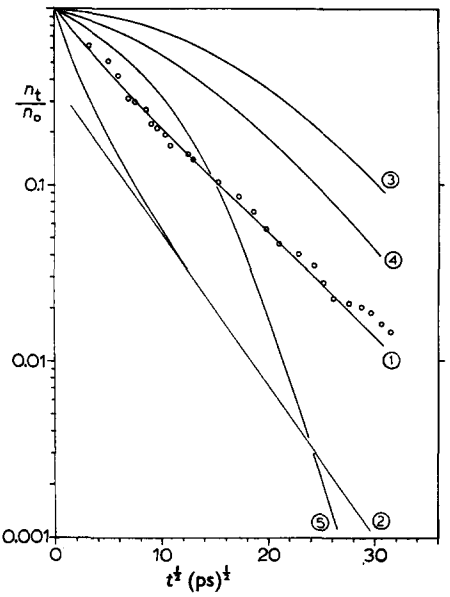

Fig. 2. Log fluorescence intensity (normalised) versus square root of time (in picoseconds$^{\frac{1}{2}}$). The data points (○) are from refs. 3 and 4 for dark adapted *Chlorella* at 10^{15} photons/pulse. The straight line through curve 2 is the quoted gradient for dark adapted *Chlorella* at $8 \cdot 10^{15}$ photons/pulse also taken from refs. 3 and 4. The smooth curves 1 and 2 are drawn from Eqn. 9 with parameters for curve 1 of $n_0 = 2.5$, $\alpha = 7 \cdot 10^4\ s^{-\frac{1}{2}}$, $\beta = 2.2 \cdot 10^5\ dm^3 \cdot m^{-1} \cdot s^{-\frac{1}{2}}$ and for curve 2, $n_0 = 40$, $\alpha = 10^5\ s^{-\frac{1}{2}}$, $\beta = 2.2 \cdot 10^5\ dm^3 \cdot m^{-1} \cdot s^{-\frac{1}{2}}$. $n_0 = 1 = 2 \cdot 10^{14}$ photons/pulse has been used to calculate curve 2 but in curve 1 half this value was used. This difference is within the experimental errors of the measurement of the number of photons/pulse. The smooth curves 3, 4 and 5 were all calculated using Eqn. 6. $n_0 = 2.5$ was used for each curve, the parameters used for curve 3 were $\alpha = 2.5 \cdot 10^9\ s^{-1}$, $\beta = 3 \cdot 10^{10}\ dm^3 \cdot m^{-1} \cdot s^{-1}$, those for curve 4 were $\alpha = 2.5 \cdot 10^9\ s^{-1}$, $\beta = 3 \cdot 10^{11}\ dm^3 \cdot m^{-1} \cdot s^{-1}$ and those used for curve 5 were $\alpha = 10^{10}\ s^{-1}$, $\beta = 3 \cdot 10^{10}\ dm^3 \cdot m^{-1} \cdot s^{-1}$.

of the quenching rate upon time arises from the fact that the existence of a certain excited molecule for a finite time without reacting not only eliminates certain possible initial quenching configurations, but also decreases the probability of quenching at later times [21, 22]. More specifically some excited states are produced close to the trap and hence trap in only a short time while others are produced some distance away and thus on average take longer to trap. The distribution of distances thus produces a time-dependent quenching rate. Eventually, the initial anisotropy of excited molecules and traps is removed and the fluorescence quenching rate becomes constant and the fluorescence decay becomes independent of time [21, 22].

In the PSU, energy migration takes the place of molecular diffusion. Furthermore, as we are dealing with a process the rate of which depends upon the inverse sixth power of distance, rather than being described by the usual laws of motion, we are unable to apply Fick's laws to calculate the diffusion coefficient for energy migration. Although the laws governing the migration and molecular diffusion are different, the effect on the fluorescence quenching is qualitatively the same and we expect the quenching rate to depend upon time, as is observed. This will be the case whether or not the lake or puddle model of the PSU is used. As only 300–500 mole-

cules are present for each trap, there is not sufficient time (or number of molecules visited) before quenching for the rate to become time independent and the fluorescence decay exponential. This effect might be more exaggerated with the puddle model, since migration is confined to such a small number of molecules. To obtain further information on this unusual type of energy migration the mean square displacement of a random walk incorporating many nearest neighbour interactions in a non-regular matrix of points has been calculated (ref. 23 and unpublished results). The displacement is proportional to the diffusion coefficient of the migration. With this information, a trapping rate dependent on time may be calculated in a similar manner to that of molecular diffusion and subsequent trapping by resonance transfer (refs. 23–25, and unpublished results).

In Fig. 2 the calculated fluorescence decays (Eq. 6, curves 3, 4 and 5) are drawn together with experimental data from picosecond fluorescence measurements [2–4], the circles are the data points for dark adapted *Chlorella* at ^{15}photons/cm^2 per pulse incident intensity and the straight line drawn through curve 2 is the gradient quoted, also for the *Chlorella*, at $8 \cdot 10^{15}$ photons/cm^2 per pulse [2]. It is clear that curves 3, 4 and 5 (from Eqn. 6) in Fig. 2 do not match the experimental data. The nature of the experimental data and the arguments outlined above suggest that time-dependent quenching process may be important.

When we include the time-dependent rates into Eqn. 1 we obtain

$$dn/dt = I(t) - an - \alpha n t^{-\frac{1}{2}} - bn^2 - \beta n^2 t^{-\frac{1}{2}}$$

where a, b and $I(t)$ are defined as before and α and β are the corresponding transient terms. This equation may be integrated directly to yield fluorescence intensity with time but further integration to give the fluorescence yield cannot be carried out in a closed form. Instead, from our knowledge of the experimental decay curves, we suggest than terms a and b are small compared to the transient terms α and β and consequently the equation is simplified to

$$dn/dt = I(t) - \alpha n t^{-\frac{1}{2}} - \beta n^2 t^{-\frac{1}{2}} \tag{8}$$

which on integrating and normalising gives $n(t)$ the fluorescence intensity at time t

$$n(t)/n(0) = \alpha/((\alpha+\beta n_0)\exp(2\alpha t^{\frac{1}{2}}) - \beta n_0) \tag{9}$$

and further integration produces the fluorescence yield Φ*.

$$\Phi = K_f/2\alpha\beta n_0 \cdot \sum_{J=1}^{\infty} 1/J^2(\beta n_0/(\alpha+\beta n_0))^J \tag{10}$$

In Fig. 1 we have plotted Φ (curve b and Eqn. 10) as a function of n_0. Also plotted are the experimental data from refs. 1, 6–8. It is found that curves A and B in Fig. 1 both describe the experimental yield versus intensity but in Fig. 2, curves 1 and 2, calculated from Eqn. 9, now describe the experimental data more accurately than curves 3, 4 or 5 which are calculated from Eqn. 6. The apparent discrepancy between the fits to the data for yields and lifetimes presumably reflects the insensitivity

* Summation over twenty terms was sufficient for convergence at this expression.

of the yield to the form of the quenching process. In Fig. 2 to match the data at different light intensities we have assumed $2 \cdot 10^{14}$ photons/cm^2 per pulse from the picosecond laser to be equivalent to 1 hit on the PSU. This figure is derived from the estimated volume of the PSU [26] and average concentration of chlorophyll present. Because of the uncertainties of these values, the number of hits at a given intensity is probably only accurate to a factor of 2. At low intensities, less than one photon per pulse is absorbed on average in each PSU. However, by assuming that a Poisson distribution describes the exact number of photons absorbed for a given average number we may correct the yield calculated from Eqn. 7 or 10 using the equation,

$$\Phi(R) = \sum_0^\infty P(R) \int_0^\infty \mathrm{d}t K_f n(R, t)/n_0$$

In this equation, n_0 is the average number of hits, R the exact number and $P(R)$ the Poisson probability. The yield corrected in this manner differs by only 2 % from that of Eqn. 9 when $n_0 < 1$ and by a smaller percentage at larger values of n_0.

The experimental fluorescence decay data are matched at various n_0 values, using Eqn. 9, by varying both α and β. The specific rate β has a value of $2.2 \cdot 10^5$ dm$^3 \cdot$ m$^{-1} \cdot$ s$^{-\frac{1}{2}}$, which is equivalent to a second-order rate constant of $5 \cdot 10^{10}$ dm$^3 \cdot$ m$^{-1} \cdot$ s^{-1}, similar to that found for chlorophyll singlet-singlet quenching [15]. The change in α necessary to fit the data at high light intensities may be explained by assuming that the triplet states are formed rapidly (< 30 ps) and that their decay is slow on the nanosecond time scale of the experiments. If this is so, then α may be increased in proportion to n_0 since the triplet concentration in Reaction 3 is constant. At low intensities [2], α is $4.7 \cdot 10^4$ s$^{-\frac{1}{2}}$ the difference between this and the α needed to match the data (10^5 s$^{-\frac{1}{2}}$) represents the pseudo first-order rate constant of the additional quenching process at high intensities.

Role of triplet states

Rather than changing the rate constant α at different light intensities, which compensates for the additional quenching produced by triplets, we have instead used Eqns. 11 to account for the time evolution of singlets and triplets.

$$\mathrm{d}n/\mathrm{d}t = I(t) - \alpha n t^{-\frac{1}{2}} - \beta n^2 t^{-\frac{1}{2}} - \gamma n m t^{-\frac{1}{2}} \qquad (11)$$

$$\mathrm{d}m/\mathrm{d}t = \varepsilon \beta n^2 t^{-\frac{1}{2}}$$

where m is the number of triplets in the PSU, γ is the singlet-triplet quenching rate constant and ε is the proportion of β that produces triplets, i.e. the branching ratio for Reactions 1 and 2. In Eqns. 11 we have used Reactions 1, 2 and 3 only. Reaction 4 may be slow as it is limited by the diffusion of the triplet states to one another which may only occur by the exchange mechanism between the T and S_0 states. In solution the T-T annihilation occurs at the diffusion controlled rate [27] ($2 \cdot 10^9$ dm$^3 \cdot$ m$^{-1} \cdot$ s^{-1}) whereas in vivo this annihilation process could only be measured in conjunction with other parameters making the value of the rate constant somewhat uncertain [28].

The equations to describe the singlet and triplet populations cannot be directly integrated in time in a closed form so we have used a variable step Runge-Kutta algorithm (Mersons method) to integrate these equations numerically. We have

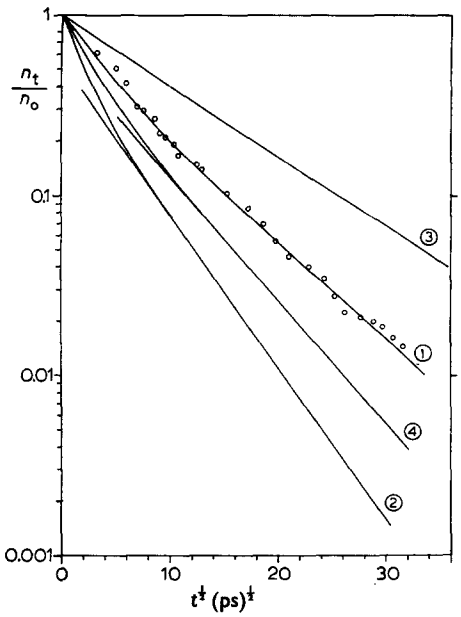

Fig. 3. Log fluorescence intensity (normalised) versus square root of time (in picoseconds$^{\frac{1}{2}}$). The data points on curve 1 are the same data as in Fig. 2 for 10^{15} photons/pulse [3, 4]. The straight line through curve 2 is the same as that in Fig. 2 for $8 \cdot 10^{15}$ photons/pulse. In curves 3 and 4 the straight lines through the curves (superimposed in the case of curve 3) refer to decays for pre-illuminated DCMU-treated chloroplasts [3, 4] at $5 \cdot 10^{14}$ and $8 \cdot 10^{15}$ photons/pulse. The smooth curves 1 and 2 are drawn from Eqn. 11 with $\beta = 9 \cdot 10^6$ dm$^3 \cdot$ m$^{-1} \cdot$ s^{-1} for each curve. The parameters for curve 1 are $n_0 = 16$, $\alpha = 4.7 \cdot 10^4$ s$^{-\frac{1}{2}}$, and for curve 2, $n_0 = 40$, $\alpha = 4.7 \cdot 10^4$ s$^{-\frac{1}{2}}$. For curve 3, $n_0 = 16$, $\alpha = 5.5 \cdot 10^8$ s^{-1} and for curve 4, $n_0 = 40$, $\alpha = 5.5 \cdot 10^8$ s^{-1}. The values for α are taken as the experimentally determined values for the decays at low light intensities [3, 4] and $\gamma = 2\beta$.

ignored the possible correlation between the quenching states produced adjacent to one another. The results of this integration are shown in Fig. 3, curves 1 and 2, along with the experimental decays of dark adapted *Chlorella* fluorescence [2] which are the straight lines drawn through the calculated curves. The gradients for these lines are from ref. 2. The same values of the parameters β and γ fit the data using the experimentally determined value [2] of α of $4.7 \cdot 10^4$ s$^{-\frac{1}{2}}$ for dark adapted *Chlorella*.

When the reaction centres are closed by 3(3,4-dichlorophenyl)-1,1-dimethylurea (DCMU) and pre-illumination, the fluorescence decay (with low intensity excitation) is exponential [2] and of 1.8 ns lifetime. This indicates that as the trap is closed the energy may migrate to an alternative trap among chlorophylls attached to another reaction centre. Alternatively, if the energy remains in the same antennae system, it must visit each chlorophyll and reaction centre trap several times before quenching since the fluorescence decay appears exponential. If this were not the case, the decay would have the same form as is observed in the dark adapted samples. When the reaction centres are closed, the intensity effects should be more pronounced than in the open state since the longer fluorescence decay times allow more extensive migration to occur. This increases the probability of excitation annihilation (assuming that the size of the PSU is the same in the open and closed states). As the annihilation rates

are unaffected by the state of the reaction centre traps, we may write the Eqns. 12 to describe the fate of the excitation:

$$dn/dt = I(t) - \alpha n - \beta n^2 t^{-\frac{1}{2}} - \gamma nmt^{-\frac{1}{2}} \qquad (12)$$
$$dm/dt = \varepsilon\, \beta n^2 t^{-\frac{1}{2}}$$

The parameters have the same meaning as before, but α is now 0.00055 ps^{-1}, the experimentally determined rate constant when the traps are closed [2–4]. These equations were integrated in the same manner as for Eqns. 11 and are also plotted in Fig. 3 as curves 3 and 4. In both cases it was necessary to adjust slightly the normalisation of the calculated curves to fit the data, but this was not a serious drawback as (a) the first 50 ps of the fluorescence decays were not time resolved [2], the gradient of the first measured part of the decays being larger than the final gradients quoted [2–4] and (b) the $t^{-\frac{1}{2}}$ time dependence does not apply below $\approx$ 10 ps, so that the calculated singlet population remains finite at $t = 0$. This last problem also arises with diffusional quenching in solution [20].

In Fig. 3, by varying n_0 only, the same parameters may be used to describe all the fluorescence decays using the appropriate experimental values for α. The parameter ε in Eqns. 11 and 12 was assumed to be equal to 0.5. Varying ε only affects the value of γ, as may be seen by inspection of Eqns. 11 and 12. Halving ε would have the effect of doubling γ to produce the same calculated curve.

Surprisingly, at high light levels the fluorescence still decays faster for dark adapted samples than for those with their traps closed. We might have anticipated that the annihilation would produce similar decays both when the traps are open or closed. It would appear that the annihilation is so efficient at reducing the singlet population that, even at intensities where many photons are absorbed in each PSU, the reaction centre becomes closed in only a few PSU's over the time scale of the measurements. This, of course, would also be the effect if it has taken tens to hundreds of picoseconds to close a trap. A second excitation would then be quenched by an effectively open trap if it arrived sufficiently soon after the first. This could occur if the first step in the closing of the reaction centre were the production of an excited state which can accept energy irreversibly from the antennae chlorophylls. This would then decay, in a short time, to another state, possibly a charged species to which Förster transfer from the antennae chlorophylls is improbable.

At low excitation intensities the experimental decays are only matched by assuming a larger value of n_0, the number of hits on the PSU, than that indicated by the number of incident photons. It seems unreasonable that the rates α, β and γ should vary with light intensity so other explanations must be sought. The purpose of the PSU's attennae is to collect and then direct the excitation energy preferentially towards the reaction centre. This may mean that at low intensities two photons absorbed in different parts of the antennae are directed towards the same few chlorophyll molecules where the probability of annihilation is increased over that assumed from the average number of photons absorbed. When many excited states are produced instantaneously in the PSU annihilation may occur after only a few jumps over neighbouring molecules. The structure of the PSU would then have less effect on the quenching of the excitation than at lower intensities where the migration is more extensive. The rapid energy transfer from chlorophyll triplets to carotenes in the antennae and the formation of chlorophyll radical ions will also contribute to

depletion of the triplet states. A more detailed model will have to take into account these processes but at present the addition parameters needed and the lack of experimental information on the time and intensity dependence of chlorophyll triplets and ions in vivo do not justify such an approach.

ACKNOWLEDGEMENTS

We wish to thank the Science Research Council for overall support of this work and G.S.B. wishes to thank the Royal Society for the award of a Mr. and Mrs. John Jaffé Donation Research Fellowship. We are also grateful to Dr. J. Breton and Dr. N. Geacintov for pre-publication copies of their papers, and to Dr. J. Peretti and Mr. C. Tredwell for stimulating discussions.

REFERENCES

1 Campillo, A., Shapiro, S., Kollman, V., Winn, K. and Hyer, R. (1976) Biophys. J. 16, 93–97
2 Porter, G., Synowiec, J. and Tredwell, C. (1977) Biochim. Biophys. Acta 459, 329–336
3 Harris, L., Porter, G., Synowiec, J. and Tredwell, C. (1976) Biochim. Biophys. Acta 449, 229–339
4 Searle, G., Barber, J., Harris, L., Porter, G. and Tredwell, C. (1977) Biochim. Biophys. Acta 459, 390–401
5 Campillo, A., Kollman, V. and Shapiro, S. (1976) Science 193, 227–229
6 Geacintov, N. and Breton, J. (1977) Biophys. J. 17, 1–15
7 Breton, J. and Geacintov, N. (1976) FEBS Lett. 69, 86–89
8 Monger, T., Cogdell, R. and Parson, W. (1976) Biochim. Biophys. Acta 449, 136–153
9 Sauer, K. (1975) in Bioenergetics of Photosynthesis (Govindjee, ed.), Academic Press, New York
10 Babenko, S., Bendereskii, N. and Lavrushko, A. (1972) Izvest. Akad. Nauk. S.S.S.R. ser fiz, 36, 1113–1116
11 Birks, J. (1973–75) in Organic Molecular Photophysics (Birks, J., ed.) Vols. I and II, Wiley
12 Hochstrasser, R. and Nelson, A. (1976) Optics Commun. 18, 361–366
13 Rahman, T. and Knox, R. (1973) Phys. Stat. Sol. 58, 715–720
14 Knox, R. and Ghosh, V. (1975) Photochem. Photobiol. 22, 149–150
15 Beddard, G. S., Carlin, S. E. and Porter, G. (1976) Chem. Phys. Lett. 43, 27–32
16 Madge, D., Windsor, M., Holten, D. and Gouterman, M. (1974) Chem. Phys. Lett. 29, 183–187
17 Beddard, G. S., Porter, G. and Tredwell, C. (1975) Nature 258, 166–168
18 Mauzerall, D. (1976) Biophys. J. 16, 87–91
19 Mauzerall, D. (1976) J. Phys. Chem. 80, 2306–2309
20 Swenberg, C., Geacintov, N. and Pope, M. (1977) Biophys. J. 16, 1447–1451
21 Noyes, R. M. (1954) J. Chem. Phys. 22, 1349–1360
22 Noyes, R. M. (1961) Progress in Reaction Kinetics (Porter, G., ed.), in Vol. 1
23 Beddard, G. S. and Porter, G. (1976) Nature 260, 366–367
24 Klein, U., Frey, R., Hauser, M. and Gösele, U. (1976) Chem. Phys. Lett. 41, 139–142
25 Yokata, M. and Tanimoto, O. (1967) J. Phys. Soc. Jap. 22, 779–784
26 Park, B. and Biggins, J. (1964) Science 144, 1009
27 Linschitz, H. and Sarkanen, K. (1958) J. Am. Chem. Soc. 80, 4826–4832
28 Stacy, W., Mar, T., Swenberg, C. and Govindjee (1971) Photochem. Photobiol. 14, 197–219